

Article

# Developing New Cleaning Strategies of Cultural Heritage Stones: Are Synergistic Combinations of a Low-Toxic Solvent Ternary Mixtures Followed by Laser the Solution?

Chiara Ricci <sup>1,2,\*</sup>, Francesca Gambino <sup>1</sup>, Marco Nervo <sup>1</sup>, Anna Piccirillo <sup>1</sup>, Arianna Scarcella <sup>1</sup>, Francesca Zenucchini <sup>1</sup> and José Santiago Pozo-Antonio <sup>2,\*</sup> 

<sup>1</sup> Fondazione Centro Conservazione e Restauro “La Venaria Reale”, 10078 Venaria Reale (TO), Italy; francesca.gambino@unito.it (F.G.); marco.nervo@centrorestaurovenaria.it (M.N.); anna.piccirillo@centrorestaurovenaria.it (A.P.); arianna.scarcella@centrorestaurovenaria.it (A.S.); francesca.zenucchini@centrorestaurovenaria.it (F.Z.)

<sup>2</sup> Dpto. Enxeñaría dos Recursos Naturais e Medio Ambiente, Escola de Enxeñaría de Minas e Enerxía, Universidade de Vigo, 36310 Vigo, Spain

\* Correspondence: cricci@uvigo.es (C.R.); ipozo@uvigo.es (J.S.P.-A.)

Received: 4 April 2020; Accepted: 8 May 2020; Published: 10 May 2020



**Abstract:** As the UN Agenda 2030 recognizes heritage protection in several goals, this research was focused on the improvement of the graffiti removal from stones. The cleaning of two graffiti paints with different composition (an alkyd- and an acrylic-based paints) from two stones (gneiss and travertine) was performed considering a synergistic approach based on the combination of a low-toxic solvent ternary mixture, followed by an Nd:YAG laser. The different concentrations of the low-toxic solvents were based on the triangular Teas graph, keeping similar Hansen solubility of the products commonly used in conservation of cultural heritage: methyl ethyl ketone (MEK) and n-butyl acetate. The n-butyl acetate was replaced by mixture A (51% ethyl alcohol/11% acetone/38% isooctane) and MEK by mixture B (7%/13%/80%). Regardless of the graffiti composition, the gneiss was satisfactorily cleaned with the mixture A, while for the travertine, the best results were achieved by the mixture B. Then, surfaces treated with the mixtures were irradiated with a QS Nd:YAG laser working at 532 nm. The cleaning evaluation was performed by stereomicroscopy, color spectrophotometry, roughness measurements, reflectance measurements, and scanning electron microscopy. As result, regardless on the stone and the graffiti paints, it was confirmed the enhancement of cleaning of the mixtures followed by the Nd:YAG laser. However, it is crucial to identify previously the concentrations of the chemical products that allow the best performance considering the graffiti-stone interaction, on the one hand, and the optimal laser's parameters, on the other hand.

**Keywords:** stone cleaning; cultural heritage; graffiti; chemical cleaning; laser; gneiss; travertine

## 1. Introduction

The UN Agenda 2030 recognizes through its Sustainable Development Goal 11 the protection of the culture and heritage as a requirement to achieve a sustainable future for humanity [1]. In its target 11.4, it is stated that the protection and safeguard of the world's cultural and natural heritage is fundamental to make cities and human settlements inclusive, safe, resilient and sustainable. Furthermore, the protection of the culture and heritage is included in other targets such as 4.7 (Education for a culture of peace and cultural diversity), 8.9 and 12.b (Sustainable tourism that promotes local culture). The International Council on Monuments and Sites (ICOMOS) recognizes Heritage to have a crucial role within the

urban development process, mainly creating social cohesion, benefits by preserving cultural resources and enhancing the appeal and creativity of regions [2]. Therefore, it is a challenge to preserve this fragile and unique heritage for current and future generations.

In parallel, graffiti represent one of the most threatening deterioration forms affecting cultural heritage materials. This form of vandalism affects more than three million of the protected monuments in Europe and therefore, millions of euros have been spent in the connected cleaning campaigns [3,4]. Consequently, for 10 years, scientific researches have been based on the assessment of the results obtained by different cleaning procedures to remove graffiti paints on stones with different texture and mineralogy (mainly granite and marble) belonging to cultural heritage of European cities [5–7]. It is well known that the most appropriate cleaning method may be selected considering both the composition of the graffiti, the chemical, mineralogical and physical properties of the stone and the state of preservation of the stone itself [7,8]. According to the deontological code of cultural heritage conservation expressed in the Venice charter [9], a cleaning treatment should not significantly modify the physical properties of treated materials, such as the color, roughness, reflectance, etc.

Among the traditional chemical and mechanical procedures to remove paint layers, both organic solvents (e.g., methylene and acetone) or alkali caustic removers and water-jet technology (e.g., *Hydrogommage*) are commonly used [5,10–17]. Moreover, in the last decades the use of laser ablation started to be investigated, achieving most of the 50% of the scientific publications based on the graffiti cleaning on stones [7]. The most used lasers in stone cleaning are the different harmonics-wavelengths of neodymium-based systems, i.e., Nd:YAG or Nd:YVO<sub>4</sub> [6,7]. Conversely to traditional methods, the use of laser shows advantages like non-mechanical contact, selectivity, and the possibility to adjust the cleaning conditions in real time [18]. However, drawbacks were also reported for each of the above-mentioned methods. For the chemical cleanings, chemical contamination was detected for procedures performed with caustic removers based in dichloro-methane, organic acids, solvents and anionic surfactants and solvents rich in potassium hydroxide [19]. Moreover, some chemical solvents, once dissolved the graffiti paint, induced the paint penetration in the substrate, resulting in a “ghosting” effect and making its removal more difficult [12,20]. For the mechanical cleaning, the use of pressurized water often originates multiple hues and loss of grains, as reported in [21] for marble surfaces. Working with laser, the cleaning effectiveness depends on material properties (i.e., absorption coefficient) and on the optimization of the laser parameters (frequency, wavelength, fluence, pulse duration, etc.) [22–24]. The selection of inappropriate parameters before to perform the cleaning could induce irreversible damages, such as fusion of the forming minerals, colorimetric changes, grain extraction [7 and references therein]. Concerning the different Nd:YAG wavelengths, Samolik et al. [13], working with a Nd:YAG laser to remove black, white, and red graffiti paints based on nitrocellulose, acrylic, and alkyd resins from limestone, sandstone, plaster, and brick, reported yellowing with first harmonic (1064 nm), darkening with 355 nm, and satisfactory results with 532 nm. Recently, Giusti et al. [20] also reported satisfactory results working with 532 nm to extract different alkyd resins as graffiti spray from a marble substrate, since they were fresh paint layers.

Despite chemical and mechanical methods and laser ablation being investigated by themselves, there are only two research papers based on the synergistic results obtained through the combination of different systems to remove graffiti paints [20,25]. In Avebury Neolithic sandstones and Stonehenge Heel, methylene dichloride and acetone, prior to laser, were successfully tested to remove the remaining paint [25]. In a recent research, Giusti et al. [20] working with a Q-switched Nd:YAG laser at 532 nm followed by chemical agents (a commercial graffiti remover in gel and methyl ethyl ketone-MEK) to remove spray paints from a marble, achieved satisfactory paint removal minimizing the risk of the colorant penetration into the fissures. The selection of cleaners must consider the toxicity of each solvent [26], as well as possible induced environmental pollution. Researches from the Italian “Istituto Superiore per la Conservazione ed il Restauro” (ISCR) have developed the open source software Trisolv<sup>®</sup> (Rome, Italy) [27,28], which is based on the triangular Teas graph and permit to mix solvents with a lower toxicity and higher Threshold Limit Value-Time-Weighted Average (TLV-TWA)

values (Table 1), although keeping similar Hansen solubility parameter values to the initial pure solvent (i.e.,  $Fd$  = dispersion force;  $Fp$  = polar force;  $Fh$  = hydrogen bonding force) [29]. The solubility parameters of mixtures can be calculated from the parameters of single solvents, multiplied by the fraction that each solvent occupies in the blend, then, the results for each solvent must be summed up to obtain the value for the mixture [30].

Following the satisfactory performances of combined methodologies reported above [20,25], in this paper, the combination of chemical products followed by an Nd:YAG laser working at 532 nm to remove two different graffiti paints from two stones with different mineralogy and texture (respectively, a gneiss and a travertine) was evaluated. The study involved a mixed group of professionals, composed of both restorers and scientists, respectively testing the cleaning procedures and assessing the effectiveness of each treatment by means of a multi-analytical protocol. An initial test allowed one to select, among some of the most commonly used solvents (ligroin, acetone, ethyl alcohol, isopropyl alcohol, MEK, n-butyl acetate, cyclohexane, ethyl lactate, and ShellSol<sup>®</sup> D40 (Kremer Pigmente GmbH & Co. KG, Aichstetten, Germany) which one achieved the best performances considering each pair paint–stone. Then, in order to avoid toxic solvents, the appropriate concentrations for a replacement low-toxic solvents ternary mixture (made of ethyl alcohol, isooctane-trimethylpentane, and acetone) were obtained using the software Trisolv<sup>®</sup> based on the triangular Teas graph. The performance of the single ternary solvents mixture was compared with the combined treatment with the laser, investigating the graffiti removal and damage induced to the surface. Therefore, appearance, color, reflectance, roughness, and micromorphology of the stones after the chemical cleanings by themselves and the combined methodology were investigated.

## 2. Materials and Methods

### 2.1. Stones

Two different lithotypes, both extensively used in the architecture of the city centre of Turin (NW Italy), were considered in the study for the preparation of mock-ups.

*Pietra di Luserna* (hereinafter called P) is an orthogneiss showing a grey-greenish coloration (Figure 1a). It is characterized by a micro-augen texture, a medium-fine grain size and high fissibility [31,32]. According to [33], and using a Micromeritics Autopore IV9500 porosimeter (Micromeritics Instruments Corporation, Atlanta, GA, USA) on three samples previously dried till constant mass, total porosity of the gneiss was measured by mercury intrusion porosimetry (MIP) and resulted to be  $0.3\% \pm 0.1\%$ . From a mineralogical point of view, P is composed by 25% mica, 30% quartz, and 40% feldspar, with epidote, chlorite and, sphene are also present as minor minerals [32]. Scanning electron microscopy with energy-dispersive X-ray spectroscopy (SEM-EDX) with two equipment, a Philips XL30 (Philips, Amsterdam, Netherlands) and a FEI Quanta 200 (Thermo Fisher Scientific, Waltham, MA, USA) in both Secondary Electron (SE) and Back Scattered Electron (BSE) modes, allowed the identification of the stone texture and the composition of the forming minerals (Figure 1b). Optimum conditions of observation were obtained at an accelerating potential of 15–20 kV, a working distance of 9–11 mm and specimen current of ~60 mA. SEM-EDX allowed the identification of the forming mineral through their EDX spectra: mica grains (Figure 1b, EDX1), quartz (Figure 1b, EDX2), and potassium feldspar (Figure 1b, EDX3). Quartz grains showed the typical stepped fracture, feldspar and biotite grains showed the exfoliation planes, laminar in the case of biotite and almost orthogonal in the case of feldspar.

*Travertine* (hereinafter called T) is a white-beige orthochemical sedimentary rock, presenting voids (Figure 1c) and, quite often, plant prints. Total porosity, measured by MIP according [33] was  $5.50\% \pm 0.5\%$ . It is completely composed by calcite (Figure 1d, EDX1). SEM-EDX allowed the identification of regular rhombohedral shape calcite grains (Figure 1d).

For each stone, seven 5 cm × 5 cm × 2 cm slabs were obtained. Considering the common surface finish found in the Turin city centre, the gneiss samples showed a flamed surface, while for travertine, the surface exhibited a disc-cutting finish.

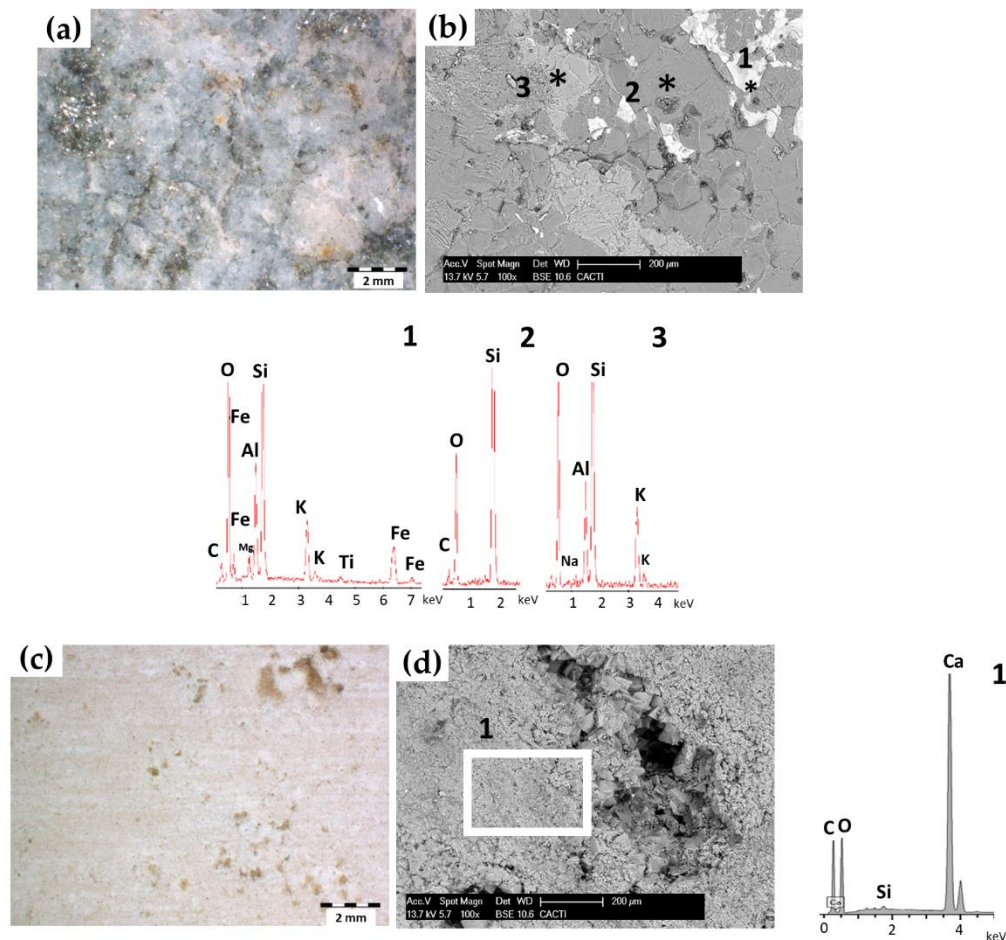


**Figure 1.** Micrographs taken with stereomicroscopy and scanning electron microscopy of the reference stones. (a,b): Gneiss. (c,d): Travertine. Moreover, energy-dispersive X-ray (EDX) spectra of the forming minerals are depicted.

## 2.2. Graffiti Paints

In order to select two graffiti paints with different composition, firstly it was performed an inventory of the graffiti paints mostly used by the writers in the city centre of Turin (NW Italy). Considering the results obtained, two graffiti paints from MONTANA Colors [34] were selected:

- a violet spray paint, the MTN94 Ultraviolet RV173;
- a green dabber paint, the MTN Street Paint Dabber UFO Green.

**Table 1.** The TLV-TWA (Threshold Limit Value-Time-Weighted Average) values expressed in ppm: a measure of the maximum amount of solvent which a worker can be safely exposed to on a daily basis for a working life (8 h/day, 40 h/week work schedule) [35].

Solvent	TLV-TWA (ppm)
n-butylacetate	50
MEK	200
2,2,4-trimethylpentane	300
acetone	500
ethyl alcohol	1000



In order to characterize the texture and the composition of the paints, both were applied on glass slides and on Parafilm<sup>®</sup> scraps (Merck KGaA, Darmstadt, Germany), a semi-transparent, flexible film composed of waxes and polyolefins.

Six slabs for each stone were covered by each paint. The surfaces were painted following [8]; the samples were painted in two phases separated by an interval of 24 h. The violet graffiti were sprayed onto the stone for 3 s at an angle of 45° and from a distance of 30 cm. The green paint was applied by means of a high flow dripper/squeezer marker.

After painting, samples were left to air-dry in the laboratory ( $15 \pm 5$  °C and  $60\% \pm 10\%$  Relative Humidity-RH) during seven days.

### 2.3. Cleaning Procedures

Prior to the combined method application (chemical cleaning followed by laser ablation), the two most suitable solvent mixtures were selected considering: (i) the solubility of the paint to be removed and the characteristic parameters of the solvents used (e.g., boiling point, flash point, toxicity, etc.) and (ii) the paint-stone interaction. In order to evaluate the solubility of the paints, some preliminary tests were made on the paints applied on glass slides. This allowed focusing on the interaction between solvent and paint, regardless of the porosity of the real substrate and the surface morphology. For this aim, either pure solvents or mixtures were tested: ligroin (a mixture of aliphatic compounds), acetone, ethyl alcohol, isopropyl alcohol, methyl ethyl ketone (MEK), n-butyl acetate, cyclohexane, ethyl lactate and ShellSol<sup>®</sup> D40 (a mixture of aromatic hydrocarbons) (Kremer Pigmente GmbH & Co. KG, Aichstetten, Germany). The two products among the above-mentioned that allowed the greatest removal of the paints from the glass slides were selected and, then, tested on stone mock-ups, in order to verify the influence of the substrate morphology and composition. The results achieved were assessed by using a stereomicroscope (OLYMPUS SZ X10, Olympus Corporation, Shinjuku, Tokyo, Japan), with digital camera OLYMPUS Color View I.

Since the aim of the research was the development of suitable strategies for the cleaning of large heritage surfaces in urban contexts (thus, outdoor and public spaces), particular attention was given to safety-related aspects. The TLV-TWA (Threshold Limit Value-Time-Weighted Average) values of the considered solvents are available online [35]. The TLV-TWA represents a measure of the maximum amount of solvent which a worker can be safely exposed to on a daily basis for a working life (8 h/day, 40 h/week work schedule); e.g., for n-butylacetate, a worker can be safely exposed to 50 ppm of this product per workable day (8 h/day) (Table 1). Instead, for solvents with lower toxicity, like ethyl alcohol, the TLV-TWA is higher (e.g., 1000 ppm).

Therefore, for each of the two selected products, an alternative ternary mixture composed by low-toxic solvents was formulated using the open source software Trisolv<sup>®</sup> [27]. These two ternary mixtures were applied on the painted stones in order to assess their effectiveness in the removal of graffiti paints. The application of both ternary mixtures on the stone was performed by means of a cotton swab, interposing a layer of Japanese paper. After a couple of minutes, the graffiti remains were removed rinsing the surface with demineralized water. Then, after one week at room conditions ( $15 \pm 5$  °C and  $60\% \pm 10\%$  RH), stereomicroscopy (OLYMPUS SZ X10) was used to assess the paint remains on the surface and, consequently, to select the ternary solvent mixture with the best performance for each paint-stone pair. Then, in order to evaluate the effectiveness of combined cleaning treatments, the treated surface with the ternary solvent mixture inducing the best performance was subjected to the laser beam application.

Considering the laser system, it was used a portable Quanta System Thunder Art laser (Quanta System S.p.A., Milan, Italy), which works at three different wavelengths (1064, 532, and 355 nm) in the Q-switched mode with a pulse duration of 8 ns. The laser output is coupled into an articulated arm. The 2nd harmonic (532 nm) was selected since in previous works, it was reported that this wavelength comparatively to the other available wavelengths, provides better performance in cleaning of graffiti paints with similar composition to those used in our research, without altering the surface [13,20].

For this laser, the pulse repetition rate could be selected from 1 to 20 Hz with energy per pulse between 100 and 350 mJ. Simulating an in situ cleaning, the manual application through a handpiece was performed. The laser beam was impinged perpendicularly onto the target surface of the specimen placed on a fix stage. A number of exploratory experiments were carried out in which the processing parameters (frequency and fluence) were changed to optimize the removal of relatively large surface areas of spray paints. As a consequence of these preliminary tests, visually evaluated under a stereomicroscopy (OLYMPUS SZ X10), repetition frequency was set to  $f = 4$  Hz and  $0.40 \text{ J/cm}^2$  keeping a distance to the target of 30 cm. The surfaces were pre wetted applying demineralized water with a cotton swab.

#### 2.4. Analytical Techniques

Previously to the paints application, scraped paints from Parafilm<sup>®</sup> scraps (Merck KGaA, Darmstadt, Germany), were analysed by Fourier transformed infrared spectroscopy (FTIR), with a FT-IR Bruker Vertex 70 (Bruker Corporation, Billerica, MA, USA). Infrared (IR) spectra were recorded at a  $4 \text{ cm}^{-1}$  resolution over 64 scans from  $400$  to  $4000 \text{ cm}^{-1}$ , in order to determine the organic base of each graffiti paints. Then, the scraped paints were investigated with X ray fluorescence (XRF) which was carried out with a  $\mu$  EDXRF Bruker ARTAX 200 (Bruker Corporation) working in the energy range 30 keV at a maximum of current of 1500  $\mu\text{A}$ . Detector has an energy resolution lower than 150 eV (Full Width Half Maximum-FWHM) for  $\text{K}\alpha$  of Mn (5.9 keV).

The painted surfaces and those treated with the ternary solvent mixtures and those treated with the combination of the chemical mixture followed by the laser were investigated with the multi-analytical protocol, based on:

- Stereomicroscopy (OLYMPUS SZ X10, with digital camera OLYMPUS Color View I) was used to evaluate the appearance of painted surfaces and the thickness and penetration of the paint layer using a cross section sample from each painted stone (a fragment of  $1 \text{ cm} \times 1 \text{ cm} \times 1 \text{ cm}$ ) embedded in resin. Moreover, stereomicroscopy was also used to identify the presence of visible paint remains on the surface
- Color spectrophotometry, using a CM-700d spectrophotometer (Minolta, Osaka, Japan) to measure the color surface of the samples before to be painted and after the cleaning. The color was measured in CIELAB color space [36]. The parameter  $L^*$  (lightness) and the polar coordinates  $a^*$  ( $+a^*$ : red;  $-a^*$ : green) and  $b^*$  ( $+b^*$ : yellow;  $-b^*$ : blue), were measured in specular component included (SCI) mode, with a spot diameter of 8 mm under the CIE standard daylight illuminant D65 at a viewing angle of  $10^\circ$ . In accordance with [37], 10 measurements were randomly taken. In order to determine the color change after the cleaning,  $\Delta L^*$ ,  $\Delta a^*$  and  $\Delta b^*$  color differences were computed considering the color of the surface before to be painted as the reference color. Then, the global color change ( $\Delta E^*_{ab}$ ) was obtained [36].
- Hyperspectral imaging was applied to determine the reflectance change of the surfaces after the cleaning. This system was applied to the unpainted stones, painted stones and the surfaces after being cleaned. The system as was reported in [16] consisted in a CCD sensor Pulnix TM-1327 GE (PULNiX America Inc., Sunnyvale, CA, USA) with an objective lens (10 mm focal length) and a spectrograph ImSpector V10 with a spectral range of 400–1000 nm and a spectral resolution of 4.55 nm. The camera scans the surface line by line to obtain an image at each of the 1040 wavelengths. A Schott DCR<sup>®</sup> III (SCHOTT-FOSTEC, LLC, NY, USA) incandescent lamp with a rectangular head of 51 mm long and 0.89 mm wide was used as a light source. A cylindrical lens placed in front of the lamp focused the light to produce an illuminated area that was 15 cm long and 1 cm wide. The sample was placed on a motorized XYZ translation stage in which the Z- axis was perpendicular to the sample surface. The  $5 \text{ cm} \times 5 \text{ cm}$  samples were fully scanned. Once the hyperspectral images were acquired, the data were processed in a MATLAB programming environment in order to display the respective reflectance graphs.

- Confocal microscopy was used to determine the roughness of the references, the painted surfaces and the treated surfaces (2 cm × 2 cm), using a P Lu 2300 Sensofar<sup>®</sup> optical imaging profiler (SENSOFAR Group, Terrassa, Barcelona, Spain). The images with the optical imaging profiler were collected with an EPI 10X-N objective, an overlapping of 25%, a depth resolution of 2 mm and a lateral resolution of 1 nm. The system allowed to obtain a 3D images of the surfaces and therefore, the roughness parameter [38],  $R_{3z}$  (third maximum peak-to-valley height) was obtained using the Gwyddion 2.47 software.
- SEM-EDX (two equipment: a Philips XL30- Philips, and a FEI Quanta 200) in BSE and SE modes was used to evaluate the chemical composition and microtexture of the painted surfaces and also, the damages induced on the surfaces after treatment. Optimal conditions of observation were the same used to characterize the stones.

### 3. Results

#### 3.1. Graffiti Paint Characterization

The FTIR analyses revealed the violet paint to have an alkyd organic base, while the green paint is an acrylic modified with styrene. The inorganic component of the paints investigated by XRF showed for both paints the presence of Ti, Si, Cl, Ca, S, and Al. Other chemical elements were found: Fe, Co, P, and K in the violet spray paint and Cu in the green dabber paint.

The observation of the painted surfaces by stereomicroscopy showed a different texture of the paint layers, depending on the finish of each stone. Regardless of the type of paint, the surface is rougher for the gneiss than for the travertine (Figure 2a,b,e,f). However, on both the gneiss and the travertine, the violet paint layer resulted to be a little thicker (20–30  $\mu\text{m}$ , Figure 3a) than the green one (5–20  $\mu\text{m}$ , Figure 3b). Both paints formed a layer following the surface morphology and did not show to penetrate into the unweathered stone substrate. In the case of travertine, both graffiti paints stuck inside the walls of voids (Figure 3b).

SEM-EDX allowed to highlight the existence of different microtextures for each paint, especially regarding the mixture and the composition. The violet paint is a C-rich matrix with microparticles with Si, Ti, and to a lesser extent Al, (Figure 2d and EDX spectrum) while the green paint showed fewer microparticles rich in Ti, Cl, Al, and Si (Figure 2h and the EDX spectrum).

#### 3.2. Cleaning Evaluation

##### 3.2.1. Selection of the Ternary Solvent Mixtures

Among ligroin (a mixture of aliphatic compounds), acetone, ethyl alcohol, isopropyl alcohol, methyl ethyl ketone (MEK), n-butyl acetate, cyclohexane, ethyl lactate and ShellSol<sup>®</sup> D40 (a mixture of aromatic hydrocarbons) the best performances, in terms of quantity of visible paint remains on the glass slide or minimum number of swipes for the cleaning, were obtained for MEK (methyl ethyl ketone) and n-butyl acetate. Then, MEK and n-butyl acetate were tested on stone mock-ups, in order to verify the influence of the surface morphology. Regardless of the graffiti paint (violet or green), n-butyl acetate showed to be the best option to clean gneiss samples, while for travertine the best results were achieved by using MEK. Both the n-butyl acetate and MEK have a TLV–TWA  $\leq 200$  ppm, thus showing a quite relevant toxicity and the convenience of finding replacement solvent mixtures (with lower toxicity but same solubility parameters). For this purpose, ethyl alcohol, acetone and 2,2,4-trimethylpentane (also known as isooctane) were mixed in different percentages, calculated by using the open source software Trisolv<sup>®</sup> [27], based on the triangular Teas graph [39]. In order to determine the percentage for each component, it has to be considered that n-butyl acetate shows  $Fd$  (dispersion force) = 60,  $Fp$  (polar force) = 13 and  $Fh$  (hydrogen bonding force) = 27 and MEK (methyl ethyl ketone) shows  $Fd$  = 53,  $Fp$  = 30, and  $Fh$  = 17 [30]. By doing so, it was possible to replace n-butyl acetate with mixture A, composed of 51% ethyl alcohol, 11% acetone and 38% 2,2,4-trimethylpentane. Mixture B, formulated

to replace MEK, consisted in 7% ethyl alcohol, 80% acetone and 13% 2,2,4-trimethylpentane (Table 2). The two mixtures were tested both on gneiss and on travertine samples. Then, the treated surfaces were evaluated by stereomicroscopy (Figure 4). For the removal of the violet paint from gneiss, similar results were detected either with mixture A or B (Figure 4, GVSa and GVSb), while in the case of the green paint from gneiss slight better results were detected on surfaces cleaned with mixture A (Figure 4, GGSa) in comparison with mixture B (Figure 4, GGSb). On the contrary, for travertine, a lower amount of paint remains was clearly identified on the surfaces cleaned with the mixture B, mainly on the surface painted with violet paint (Figure 4, TVSa and TVSb).

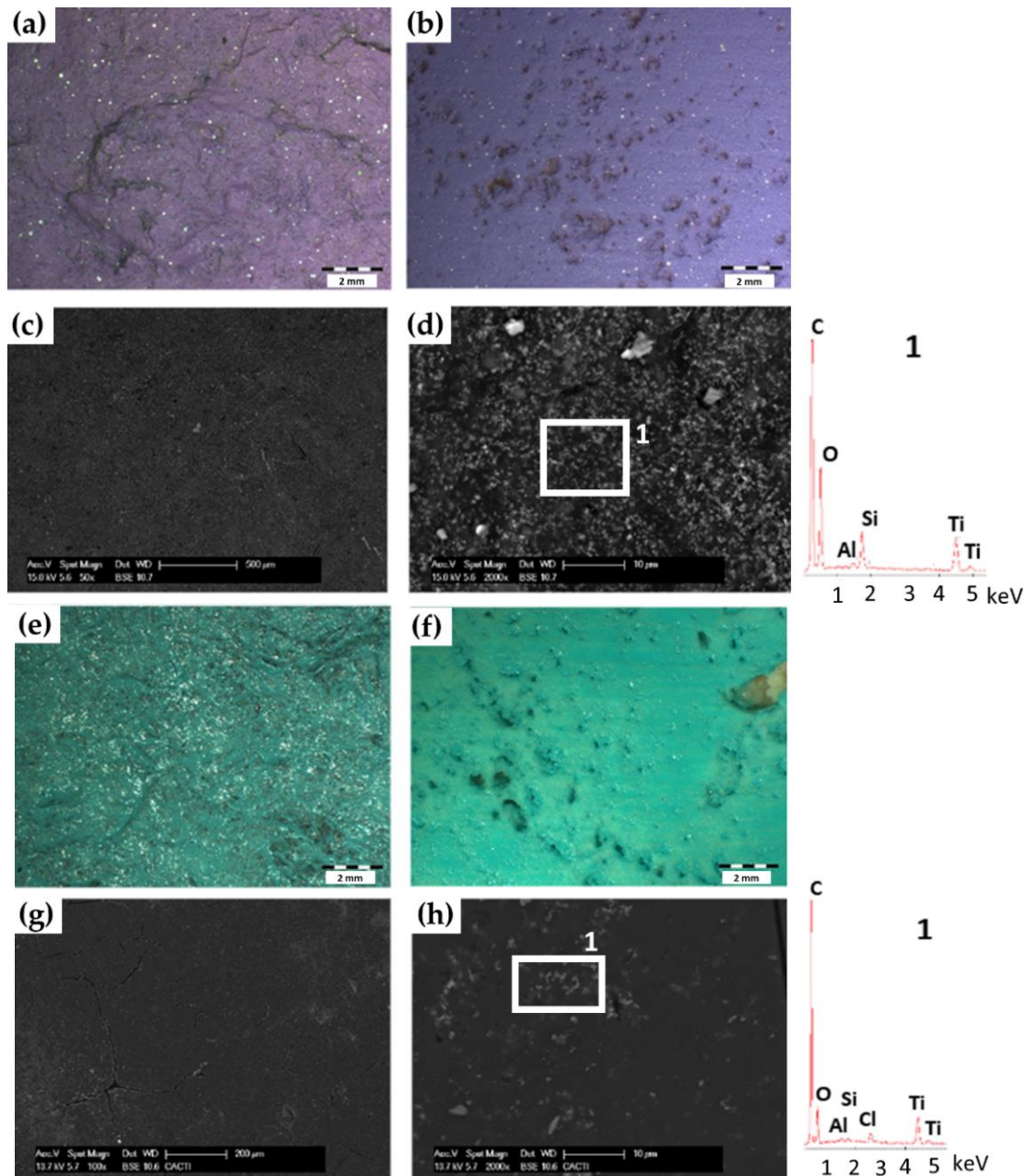


**Figure 2.** Micrographs taken with stereomicroscopy and scanning electron microscopy of stones painted with violet (a,c,d: gneiss, b: travertine) and green (e,g,h: gneiss, f: travertine) graffiti paints. EDX spectra of the paints are also shown.



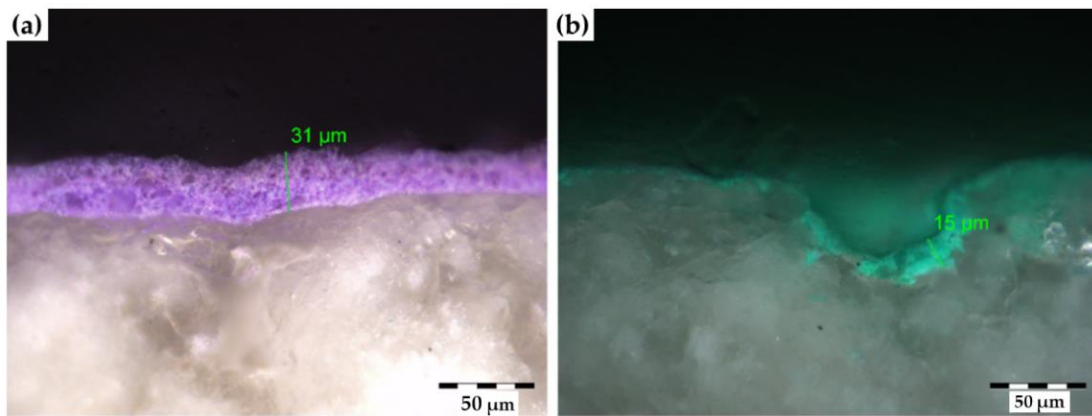


**Figure 3.** Micrographs taken by stereomicroscope of the cross sections of the painted samples of travertine. (a) Violet paint. (b) Green paint.

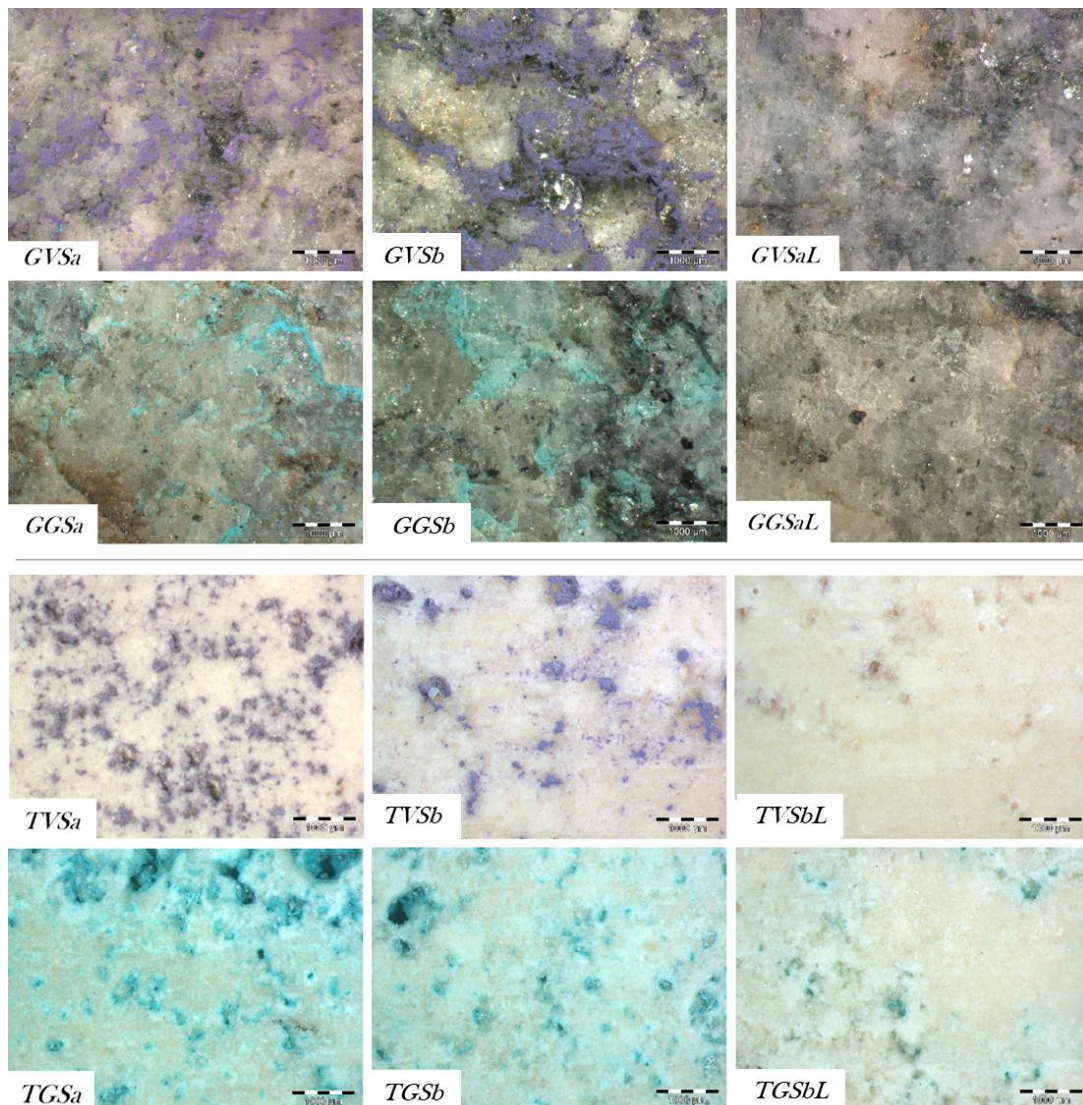


**Figure 4.** Micrographs of the cleaned surfaces taken by the stereomicroscope. Check Table 3 for sample labels.

**Table 2.** Composition (% concentration) of the two solvent mixtures tested (Mixtures A and B).

Mixture	Solvent Replaced	Ethyl Alcohol	Acetone	2,2,4-Trimethylpentane
Mixture A	n-butyl acetate	51%	11%	38%
Mixture B	MEK	7%	80%	13%

**Table 3.** Samples set up for cleaning tests in the present work. Acronyms for each sample are listed (the first letter indicating the type of stone, the second letter the type of graffiti paint and the following the cleaning treatment applied).

Stone	Color Paint	Cleaning Method	Acronym
Gneiss	–	None (stone reference)	G
		Solvent A	GVSa
		Solvent B	GVSb
	Violet	Solvent A+ laser (532 nm)	GVSaL
		Solvent A	GGSa
		Solvent B	GG Sb
		Solvent A+ laser (532 nm)	GGSaL
Travertine	–	None (stone reference)	T
		Solvent A	TVSa
		Solvent B	TVSb
	Violet	Solvent B+ laser (532 nm)	TVSbL
		Solvent A	TGSa
		Solvent B	TGSb
		Solvent B+ laser (532 nm)	TGSbL

Therefore, in order to test the combined approach with the laser, the mixture A was selected to remove graffiti from gneiss and the mixture B to clean travertine samples. The nomenclature for each sample is shown in Table 3.

### 3.2.2. Evaluation of the Surfaces Treated with the Ternary Solvent Mixtures followed by 532 nm

Compared to the chemical cleaning procedures, by using the mixture A for gneiss (Figure 4, GVSa and GGSa) and the mixture B for travertine (Figure 4, TVSb and TGSb), the treatments combining these solvent mixtures and the laser Nd:YAG working at 532 nm achieved a notable improvement in terms of effectiveness in the removal of graffiti paints.

Figure 4, captured by the stereomicroscope, shows that the combined methodology based on the use of solvents mixture A followed by laser seemed to achieve the total removal of the green paint (Figure 4, GGSaL) and almost the complete removal of the violet paint (Figure 4, GVSaL). On the GVSaL surface, violet shadows were visible on the white feldspar grains.

For travertine, despite the combined methodology also allowed an improvement of cleaning results comparatively to the solvent mixture B by itself (Figure 4, TVSb and TGSb), a difference between the two graffiti paints was highlighted: the observation by stereomicroscope allowed to identify fewer violet paint remains on the surfaces (Figure 4, TVSbL) than green paint ones (Figure 4, TGSbL). Regardless of the color, as expected, the paints remains were found to fill the characteristic voids of travertine.

Color spectrophotometry data (Table 4) allowed to identify the  $a^*$  as the parameter affecting the most color change in travertine samples. For surfaces painted with the violet spray (TVSb and TVSbL),  $a^*$  increased (increase of reddish coloration), while for those painted with the green paint (TGSa and TGSaL),  $a^*$  exhibited a decrease (trend to greenish coloration all over the surface).

**Table 4.** Mean values and standard deviation values of color coordinates  $L^*$ ,  $a^*$ , and  $b^*$  for gneiss and travertine surfaces (respectively for the reference stones and the surfaces after each cleaning treatment tested in this research for the removal of the violet and green paints). Moreover, the colorimetric differences are also shown, considering the color of the surfaces before to be painted as the reference color. Check Table 3 for sample labels.

GNEISS	$L^*$	$a^*$	$b^*$	$\Delta L^*$	$\Delta a^*$	$\Delta b^*$
G	62.45 ± 3.25	−1.20 ± 0.44	2.69 ± 1.33	–	–	–
GVSa	57.36 ± 4.84	1.00 ± 0.83	−4.01 ± 1.84	−5.09	2.21	−6.70
GVSaL	58.77 ± 2.85	−0.48 ± 0.37	−0.44 ± 0.59	−3.68	0.72	−3.13
GGSa	54.20 ± 4.39	−6.36 ± 1.24	3.44 ± 0.17	−8.25	−5.16	0.74
GGSaL	61.46 ± 2.48	−2.21 ± 0.09	1.95 ± 0.43	−1.00	−1.01	−0.74
TRAVERTINE	$L^*$	$a^*$	$b^*$	$\Delta L^*$	$\Delta a^*$	$\Delta b^*$
T	82.05 ± 1.11	2.01 ± 0.25	9.19 ± 1.75	–	–	–
TVSb	80.62 ± 0.12	3.65 ± 0.03	7.88 ± 0.36	−1.43	1.64	−1.31
TVSbL	81.63 ± 0.01	3.07 ± 0.01	9.86 ± 0.01	−0.42	1.06	0.67
TGSb	78.44 ± 0.01	−9.52 ± 0.01	8.33 ± 0.01	−3.61	−11.53	−0.86
TGSbL	82.14 ± 0.07	−1.12 ± 0.02	8.60 ± 0.02	0.09	−3.13	−0.59

For gneiss surfaces, instead, the parameters affecting the most the color change were different from case to case: (i) the treatment with mixture A of an area painted with violet spray (GVSa) induced a decrease of the  $b^*$  value (increase of blue tones); (ii) both in the case of the cleaning of violet paint with a combined use of the mixture A followed by the laser (GVSaL) and the cleaning of the green paint with mixture A (GGSa), the parameter  $L^*$  showed the highest variation; its decreasing suggesting a darkening of the surface; and (iii) the combined approach for the removal of the green paint with the mixture A followed by laser (GGSaL) induced a comparable decrease for both  $L^*$  and  $a^*$ , suggesting a darkening on the one hand, and a trend to a greenish coloration on the other hand.

Generally, for all the treated areas, except for the removal of the green paint from travertine by the combined methodology (TGSbL),  $L^*$  decreased (darkening). Moreover, the presence of paint remains on the surface after the cleaning treatment can explain the increase of  $a^*$  for samples painted with the violet spray (suggesting an increase of the red component in the global perception of the surface). The same explanation can be provided for the decrease of  $a^*$  for surfaces with green paint (increase of the greenish coloration). Both for the violet and green painted samples, the parameter  $b^*$  proved to decrease in most of the cases (GVSa, GVSaL, GGSaL, TVSb, TGSb, and TGSbL), showing a trend to a blueish coloration; the only exceptions were GGSa (mixture A for the removal of green paint from gneiss) and TVSbL (combined methodology for the cleaning of travertine surfaces painted with violet spray).

The global color change  $\Delta E^*_{ab}$  (Figure 5), considering that the lower the  $\Delta E^*_{ab}$ , the higher the cleaning effectiveness, showed an enhancement of the effectiveness of the combined cleaning methodology: in fact, the  $\Delta E^*_{ab}$  values were remarkably lower for those cases in which the use of chemicals was followed by the laser than those registered on the surfaces treated only with the ternary solvent mixture. The application of the combined methodology on gneiss for the removal of the green paint (GGSaL) and for the cleaning of both paints from travertine (TVSbL and TGSbL) achieved  $\Delta E^*_{ab}$  lower than 3.5 CIELAB units, thus suggesting a change in the visual perception of the surface not observed by an unexperienced human eye [40]. Finally, for the cleaning of violet paint from gneiss, the  $\Delta E^*_{ab}$  calculated after the application of the combined methodology (GVSaL) resulted greater than 3.5 CIELAB units (therefore clearly visible), although lower than for the cleaning with only the solvent mixture (GVSa).

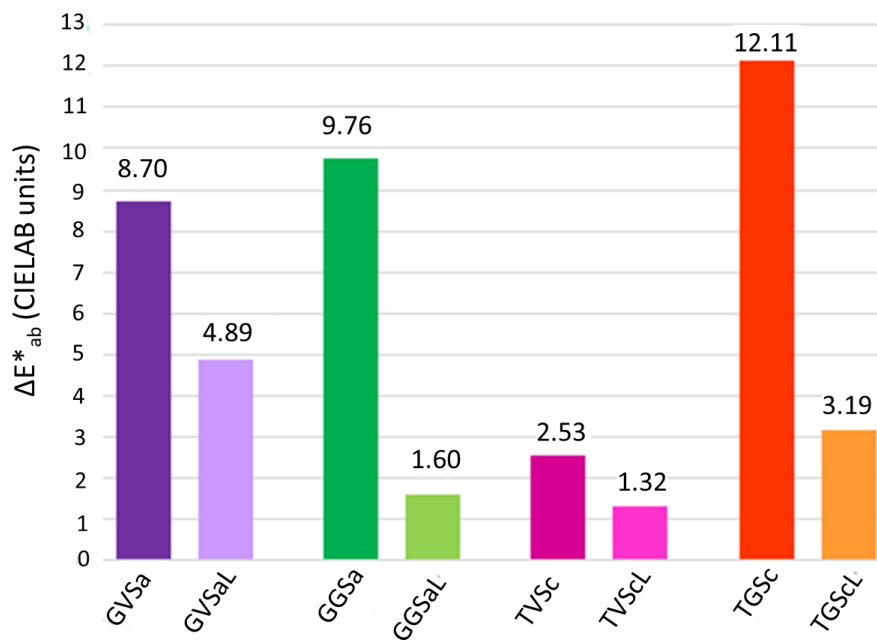


**Figure 5.**  $\Delta E^*_{ab}$  (CIELAB units) for gneiss and travertine surfaces after being treated either with a solvent mixture or the combined methodology based on the use of the solvent mixture followed by the laser working at 532 nm.  $\Delta E^*_{ab}$  was computed considering the color of the surface before to be painted as the reference. Check Table 3 for sample labels.

In order to evaluate the potential of these cleaning methodologies in inducing alterations or damages to the heritage stones, the incompatibility assessment rate based on the  $\Delta E^*_{ab}$  and proposed in [41] was applied. This methodology allows the classification of each product or procedure in three levels of risk associated to several indicators; concerning the global color change: low risk ( $\Delta E^*_{ab} < 3$ ), medium risk ( $3 < \Delta E^*_{ab} < 5$ ), and high risk ( $\Delta E^*_{ab} > 5$ ). Therefore, for both the gneiss painted with green graffiti (GGSaL) and the travertine painted with violet paint (TVSbL), whose  $\Delta E^*_{ab} < 3$  CIELAB units, the combined methodologies induced a low risk. Instead, the application of the combined cleaning treatment for the removal of the violet paint from gneiss (GVSaL) and of the green paint from travertine (TGSbL) induced a medium risk of incompatibility. Then, it is important to highlight that, in all cases, the application of the laser after the chemical cleaning notably reduced the negative effects of the solvent mixtures by themselves in terms of color modification due to the paint remains on the surfaces. The only exception resulted for the travertine painted with violet graffiti, since the surface cleaned only with the solvent mixture (TVSb) already showed a  $\Delta E^*_{ab}$  lower than 3 CIELAB units ( $\Delta E^*_{ab} = 2.53$  CIELAB units).

Figure 6 reports the reflectance spectra of the painted gneiss and travertine surfaces, both before and after being treated with different cleaning procedures, as well as the reflectance spectra of the unpainted stones (references). Looking at the reflectance spectra, it was noticed that both stones, when unpainted, showed higher reflectance than after the application of a graffiti paint (both the violet and the green), as well as after any cleaning treatment. This was true for the application both of a chemical cleaning by itself (mixture A or B) and of combined methodologies (the ternary solvent mixture followed by laser).

Concerning the reference stones, gneiss (G, Figure 6a,b) showed a constant reflectance in the measured range (450–670 nm), while travertine (T, Figure 6c,d) showed an increase of reflectance along the visible spectrum, being more intense in the red edge of the spectrum (>625 nm).



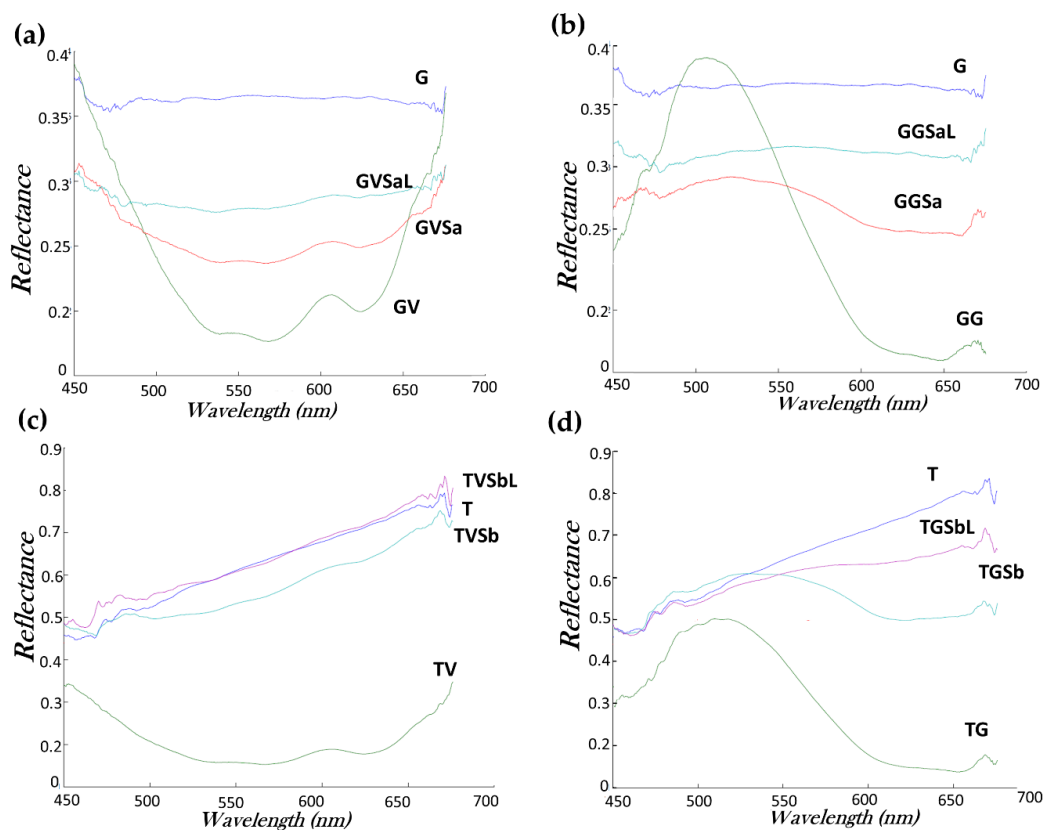


**Figure 6.** Reflectance spectra of the treated surfaces (gneiss and travertine) after the application of the cleaning procedures tested to remove violet and green paints. For comparative purposes, the reflectance spectra of the painted (GV: gneiss with violet paint; GG: gneiss with green paint; TV: travertine with violet paint; TG: travertine with green paint), and unpainted stones (G: gneiss; T: travertine) are also shown. (a) Reflectance spectra of the gneiss painted with violet graffiti. (b) Reflectance spectra of the gneiss painted with green graffiti. (c) Reflectance spectra of the travertine painted with violet graffiti. (d) Reflectance spectra of the travertine painted with green graffiti. Check Table 3 for sample labels.

As for the reflectance spectra of the painted surfaces, the violet paint (Figure 6a,c) showed an important absorption band in the range 470–650 nm, with low intensity reflectance bands at 575 and 620 nm. For the green paint (Figure 6b,d), a very intense reflectance band was observed in the range 450–600 nm (Figure 6b,d). Please notice that, in Figure 6, different shapes presented by the spectra of the same paint applied on each stones are due to the reflectance intensity of each graph (on  $y$  axis): in the spectra related to the gneiss, reflectance is scaled up to 0.4, while for the travertine, because of its higher reflectance compared to the gneiss, the reflectance scale ( $y$  axis) is considered up to 0.9.

Considering the cleaning effectiveness, the surfaces for which a higher level of cleaning is reached should be those showing a reflectance spectrum more similar (in terms of absorption and reflectance bands) and closer to the one obtained for the reference surfaces. Indeed, the surfaces cleaned with the combined methodology exhibited a reflectance closer to the reference stone. Furthermore, it is important to highlight that for the cleaning of violet paint from travertine with the combined methodology (TVSbL, Figure 6c) a higher reflectance was detected in some range of the spectrum (respectively 450–500 nm and 600–670 nm), showing maybe the beginning of damage on the surface due to a too extensive cleaning.

Roughness values ( $R_{3z}$ ,  $\mu\text{m}$ ) measured for the references stones, the painted surfaces and the different cleaning areas treated with both the solvent mixtures and the combined methodology (use of chemical products followed by the laser) are depicted in Figure 7. As it can be observed, despite the presence of voids on its surface, the travertine (T) resulted smoother than the gneiss (G).

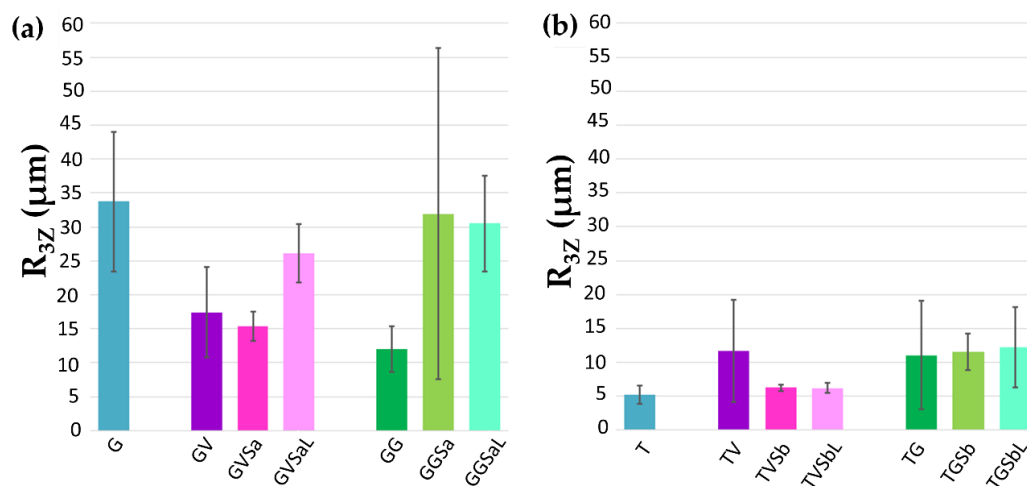


**Figure 7.**  $R_{3z}$  ( $\mu\text{m}$ ) of the reference stones (G: gneiss; T: travertine), the painted surfaces (GV: gneiss with violet paint; GG: gneiss with green paint; TV: travertine with violet paint; TG: travertine with green paint) and the surfaces treated with the different cleaning methods: respectively, the use of solvent mixtures and a combined methodology, based on the chemical cleaning followed by the laser. (a) Gneiss samples. (b) Travertine samples. Standard deviation values are also shown. Check Table 3 for sample labels.

After the application of the paints on the surfaces, two different trends were identified depending on the substrate: for gneiss, the painted surfaces (GV, GG) proved to be smoother than the unpainted stone (G). On the contrary, in the case of travertine the painted surfaces (TV, TG) had higher roughness than the unpainted one (T), although there were not statistically significant differences.

Considering the cleaned surfaces, different trends have been found:

- For the removal of the violet graffiti from the gneiss, a surface smoother than the reference stone was obtained after the application of the chemical procedure (GVSa), while for the combined treatment (GVSaL) the measured roughness resulted closer to that of the reference (G) (Figure 7a).
- For the cleaning of both the green graffiti from the gneiss and the violet spray from the travertine, all the cleaning methodologies tested (GGSa, GGSaL, TVSb, and TVSbL) produced a roughness closer to the value of the stone reference (G, T respectively) than to the painted stone (Figure 7a,b). However, in the case of the gneiss cleaned from the green graffiti with the combined methodology (GGSaL), a high standard deviation suggested the high variability of the surface roughness.
- For the travertine cleaned from the green graffiti, both cleaning procedures (TGSb, TGSbL) induced surfaces rougher than the reference (T) (Figure 7b).

A more detailed analysis with SEM–EDX allowed, on the one hand, to observe the presence of paint remains on the surface, particularly through the fissures and voids of the surface and, on the other hand, to identify possible damages induced to the stone, such as physical changes of the forming minerals (i.e., fusion and extraction of the mineral grains) or chemical contamination. For both stones (gneiss: Figure 8 and travertine: Figure 9) the cleaning procedure based on the use of a ternary low-toxic solvent mixture left on the surface a greater amount of graffiti remains than for areas treated with the combined methodology. The paint remains, pointed out with rectangles respectively in Figures 8 and 9, were identified as C-matrix deposits with Ti, S, Cl, and P, as revealed by their EDX spectra. In addition to those deposits rich in C, it was possible to observe accumulations of high contrast fine particles rich in Ti (Figure 8, GGSa). Those Ti-rich accumulations were found also on areas where the use of laser followed the chemical cleaning, even if in smaller quantities.

Concerning the surfaces cleaned with the combined methodology, a satisfactory result in the removal of the graffiti paints was achieved both for gneiss and travertine, although some remains of the green paint were still found into fissures of the gneiss (GGSaL) and in some voids of the travertine

(TGSbL). However, for the latter, the amount of graffiti paint remains found was noticeably lower than for surfaces treated with only the solvents mixture (Figure 9).

With regard to the damages possibly induced to the forming minerals, a low-intensity melting of edges of the biotite exfoliation planes was identified, as showed by arrows of Figure 8 for the sample GVSaL. For travertine surfaces, no clear damages to the calcite grains were identified (Figure 9).

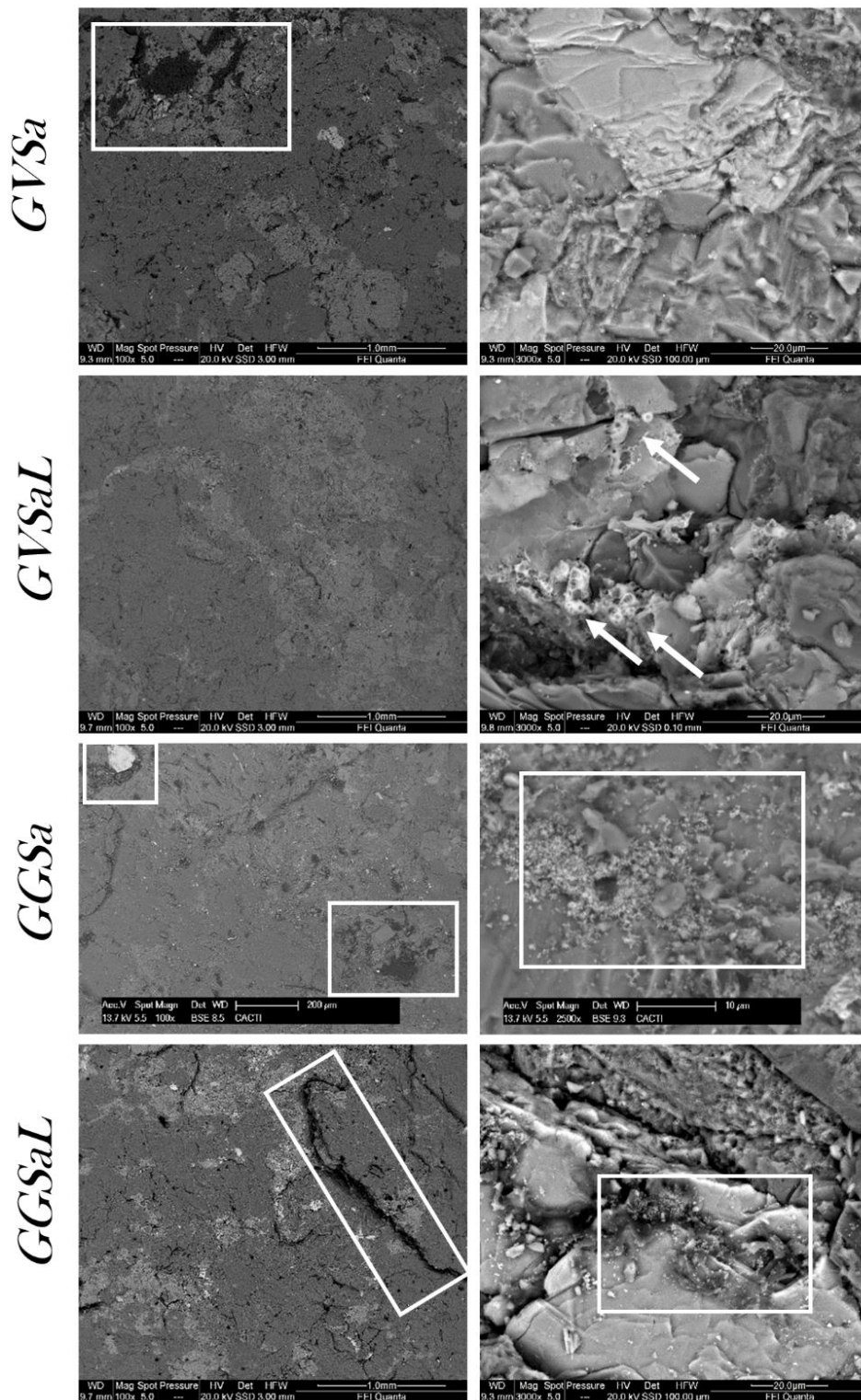


**Figure 8.** Scanning electron microscopy (SEM) micrographs of the gneiss surfaces after the application of the cleaning methods tested. Check Table 3 for sample labels.



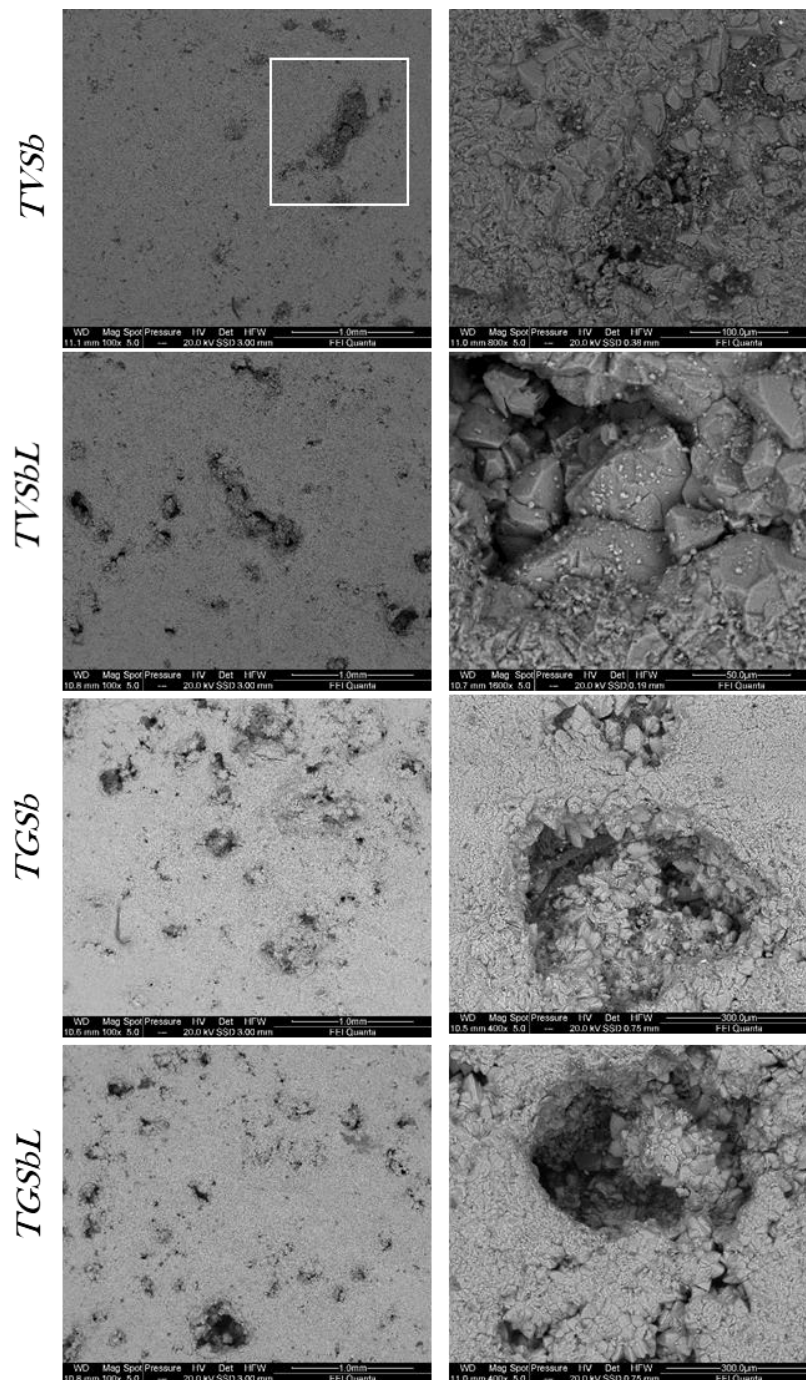


**Figure 9.** Scanning electron microscopy (SEM) micrographs of the travertine surfaces after the application of the cleaning methods tested. Check Table 3 for sample labels.

#### 4. Discussion

In this research, different cleaning procedures based either on the use of low-toxic ternary solvent mixtures (mixture A and B) or on their combination with a laser Nd:YAG working at 532 nm, were tested for the removal of graffiti paints from stones commonly found in cultural heritage in the historical city centre of Turin (Italy). Two different graffiti paints (one alkyd-based and the other acrylic-based) were considered, as well as two stones, characterized by different mineralogy, texture, and surface finish: a gneiss and a travertine.



Firstly, the best chemical products for the removal of graffiti paints from a glass slide were selected from a list of pure solvents or mixtures commonly used in the conservation field: ligroin (a mixture of aliphatic compounds), acetone, ethyl alcohol, isopropyl alcohol, methyl ethyl ketone (MEK), n-butyl acetate, cyclohexane, ethyl lactate and ShellSol® D40 (a mixture of aromatic hydrocarbons). The best performances in terms of graffiti removal from the glass slides were assessed by stereomicroscopy and proved to be those with MEK and n-butyl acetate. Cremonesi [39] reported that both those two products are characterized by good penetration and volatility and medium–high polarity, thus resulting as suitable cleaning products for most synthetic resins. Giusti et al. [20] working on the cleaning of graffiti from a marble, also detected that MEK achieved better removal results than a commercial product composed of fatty alcohol ethoxylate (1%–5%), oleic amine ethoxylate (2.5%–5%), propylene carbonate (9%–20%) and dipropylene glycol monomethylether (50%–80%). However, unlike in the current research, they reported that a complete graffiti removal was not achieved with only the use of MEK. Then, considering that both solvents are quite toxic, with TLV–TWA < 200 ppm (maximum amount of solvent that a worker can be safely exposed to on a daily basis for a working life, [35]), the open source software Trisolv® [27] was used to formulate replacement mixtures composed of three common solvents with low toxicity levels (ethyl alcohol, acetone, and 2,2,4-trimethylpentane or also called isooctane). The (*v/v*) % concentration for each of the three solvents was calculated by making sure to consider their fractional solubility parameters [30]: *Fd* (dispersion force—Van der Waals or instant dipole), *Fp* (polar force) and *Fh* (hydrogen bonding force). Thus, n-butyl acetate was replaced by mixture A (51% ethyl alcohol, 11% acetone, and 38% 2,2,4-trimethylpentane) and MEK by mixture B (7% ethyl alcohol, 80% acetone, and 13% 2,2,4-trimethylpentane). Then, the cleaning of the two graffiti (the violet alkyd paint and the green acrylic paint) from both stones was performed with both low-toxic ternary solvent mixtures, using a cotton swab and interposing a Japanese paper layer.

Finally, for each stone + paint pair the use of the solvent mixture with the best performance was combined with the Nd:YAG laser working at 532 nm, in order to determine the possible enhancement of the cleaning results (considering the improvement of the graffiti paint removal, without damaging the stone). Regarding the chemical cleaning procedures, neither the mixture A on the gneiss nor the mixture B on the travertine achieved a complete removal of the graffiti paints.

Since, as known from the literature [12,20], the ghosting may be one of the main drawbacks of chemical cleaning, a layer of Japanese paper was interposed before applying the solvent, in order to reduce the solvent penetration and the graffiti dissolution. However, the mechanical action of the cotton swab through the Japanese paper might have been insufficient, thus explaining the limited effectiveness of the cleaning.

Furthermore, the different chemical composition of the graffiti paints (respectively, alkyd- and acrylic-based) showed not to significantly affect the result. Instead, the composition of the ternary solvent mixture, as well as the paint-stone interaction (influenced by the surface finish and the fissural system of the substrate), proved to be of great relevance. Indeed, for gneiss, whose texture is characterized by three different fissures systems (transgranular, intergranular, and intragranular), the graffiti paint penetration is facilitated. On the contrary, the lack of a fissure system in travertine prevents the paint to be retained on the surface, except for the paint penetrating into the isolated voids. Besides, the higher adherence of the paint to the surface due to the presence of fissures in the substrate was found also in [17]. In that work, the cleaning effectiveness achieved by using soft-abrasive blasting technologies to remove graffiti was compared between a granite (with a bush-hammering surface) and a limestone (with a disc-cutting surface).

Moreover, as mentioned above, the composition of the two ternary solvent mixtures (different concentrations of the three solvents, i.e., ethyl alcohol, acetone, and isooctane) was decisive in determining which one was the most effective respectively for the cleaning of gneiss (mixture A) and travertine (mixture B). In particular, the former showed a lower content of acetone (11%) than the latter (80%). It is well known that acetone is a solvent characterized by an extremely rapid evaporation rate and a low flash point [30]. Therefore, it is not surprising that for gneiss samples on which the

graffiti paint showed higher adherence to the surface fissures, the mixture A was the one that worked better (in fact, the lowest is the acetone concentration, the longer could be the contact time between the paint and the solvent). The action of acetone was associated to the one of isooctane (an aliphatic hydrocarbon) and ethyl alcohol, respectively convenient for the dissolution of organic matter (e.g., oils, waxes, and paraffin) and natural resins [30,39].

Concerning the results obtained by the combined methodology, all analytical techniques (stereomicroscopy, color spectrophotometry, hyperspectral imaging, and SEM-EDX) confirmed an enhancement of the cleaning effectiveness, if compared with the results of the standalone chemical cleaning procedure. An improvement of results obtained thanks to a combined approach were recently reported also in [20], although they first used the laser, in order to achieve a thinning of the paint layer, and secondly the chemical products.

Nevertheless, the graffiti removal from the surface was still not fully effective. SEM-EDX allowed the identification of some paint remains on the surfaces (although in lower quantity than for the areas cleaned only with the solvent mixture), filling either the superficial fissures on gneiss or the voids on travertine. These graffiti paint remains were characterized as a dense and voluminous C-rich matrix, with Ti and, as minor elements, S and Cl. Titanium from rutile ( $\text{TiO}_2$ ), which is a stable phase [42], is commonly used as extender, brightener, or opacifier in paints [43,44]. SEM-EDX analyses clearly showed the presence of agglomerations of Ti-rich nanoparticles mainly on the surfaces cleaned with the solvent ternary mixtures, while the extent of these accumulations seemed to be reduced after the application of the laser. Giusti et al. [20], while cleaning alkyd graffiti paints on marble, also found an evident depletion of titanium net counts applying a combined method (laser cleaning followed by the use of chemical products) rather than only standalone chemical cleaning procedures. Therefore, we can deduce that the latter acted on the dissolution of the organic base of the paint (either alkyd or acrylic base), while allowing an enrichment of the compounds used as extenders and opacifiers.  $\text{TiO}_2$  nanoparticles tend spontaneously to form agglomeration in a suspension due to the electrostatic and van der Waals interactions [45]. The agglomeration can show sizes of hundreds of nm.

Color spectrophotometry also confirmed the highest effectiveness of the combined methodology by showing the most relevant reduction of the color changes, if compared to those detected on the surfaces cleaned only with the chemical products. In fact, considering the scale proposed in [41], the combined methodology reduced the intervention risk on heritage materials.

As for the roughness measurements, the collected data showed that, comparatively to the unpainted surface, the application of the graffiti paint (regardless of its chemical composition) induced smoother surfaces in the case of gneiss, while for travertine an increase of the surface roughness was recorded. This might be related to two facts: i) the roughness parameter measured ( $R_{3z}$ ) and ii) the initial surface finish of both stones. On the one hand,  $R_{3z}$  is the third maximum peak-to-valley height and, following [38], it is the mean value of the vertical distances of the third highest peak to the third lowest valley of the roughness profile of the sample over the evaluation length. Therefore, the deepest valley due to the presence of voids in the travertine were not considered in the computation. On the other hand, gneiss showed a flamed surface, while the travertine exhibited a disc-cutting surface. Therefore, since not considering the intrinsic presence of voids of the travertine, the surface of the latter results smoother than that of the surface of the gneiss, as shown by the roughness measurements. As a consequence, the presence of the graffiti paint acted as a smoothing agent on the gneiss, due to the filling of the initial roughness, while in the case of travertine, the intrinsic roughness of the paint was higher than that of the roughness of the substrate itself. SEM allowed the identification of paint layers composed mainly by  $\text{TiO}_2$  nanoparticles protruding in a C-matrix. For all the stone-paint pairs (except for the gneiss with violet paint), the roughness measured after the cleaning treatment (with both the use of the single solvent mixture and the combined methodology), was similar to that of the unpainted counterparts since the differences obtained between the cleaned surfaces and the references were not statistically significant. In detail, for the gneiss samples, the treated surfaces showed a roughness slightly lower than the reference, induced by the presence of paint filling fissures, as observed by SEM.

Instead, on the travertine,  $R_{3z}$  values were slightly higher than the references, due to the voluminous paint remains on the surface. Therefore, it may be highlighted the influence of the texture and surface finish on the roughness measurements after cleaning. Thus, as reported in a previous work using mechanical methods [17], it was confirmed that the presence of graffiti remains affected the variation of roughness after the cleaning treatment.

With regard to the possible harmful effects caused by the cleaning treatments to the surfaces, no drawbacks (such as calcite grain extraction) were identified on the travertine. Instead, on the gneiss, a low intense melting of the edges of the exfoliation planes of the biotite grains were identified by SEM observation. Biotite is the most critical forming mineral in the gneiss, as was reported in other researches working with granitic stones [46,47]. This is due to the relatively high optical absorption of biotite at the tested wavelength, to its pronounced cleavage and the relatively low melting temperature (about 650 °C, according to what reported in [48]).

## 5. Conclusions

Since the UN Agenda 2030 recognizes, through its Sustainable Development Goals 11, 4, 8, and 12, the protection of the cultural heritage as a requirement for sustainable future scenarios and strategies focused on the conservation of heritage elements have to be improved and fostered. Furthermore, aiming at sustainability, those conservation strategies should be as much respectful as possible toward the environment, the people and the constitutive materials of the monuments and heritage architecture.

The combined cleaning of graffiti, based on the initial application of a low-toxic solvent ternary mixture followed by an Nd:YAG working at 532 nm, achieved highest extraction level of graffiti paints than those obtained only by the ternary solvent mixtures. The satisfactory cleaning level achieved was due to an initial partial removal of the paint layer using the low-toxic ternary solvent mixture, then ensuring a moderate application of laser ablation, which improved the final result, removing most of the paint remains, except those into the fissures in the gneiss and the voids in the travertine.

Attending to the selection of the low-toxic ternary solvent mixture, the most appropriate concentrations of the low-toxic solvents (ethyl alcohol, acetone and 2,2,4-trimethylpentane) were calculated in order to obtain a mixture with solubility parameters ( $Fd$ ,  $Fp$ , and  $Fh$ ) suitable for the paint to be removed. It was verified that the most effective concentrations for the solvent mixture depended mainly on the stone underneath (fissure system and surface finish) and at lesser extent on the paint composition. The solvent mixture with the higher acetone content was selected for the cleaning of the stone substrate without a fissure system, while the mixture with the lower acetone content proved to be suitable to remove the graffiti paint when presumably more adherent to the stone, due to its penetration though superficial fissures.

In all cases, the combined methodology proved to be a low or medium-risk cleaning procedure, causing no damages on travertine surfaces and only a low-intensity melting of the edges of biotite grains for gneiss. Further studies should be done in order to minimize the melting of the biotite due to the laser application.

**Author Contributions:** Conceptualization, M.N. and A.P.; methodology, M.N., A.P., C.R., F.G., A.S., F.Z. and J.S.P.-A.; software, M.N. and J.S.P.-A.; validation, M.N., A.P., A.S. and J.S.P.-A.; formal analysis, M.N. and J.S.P.-A.; investigation, C.R., F.G., M.N., A.P. and J.S.P.-A.; resources, M.N. and J.S.P.-A.; data curation, C.R., F.G., M.N., A.P. and J.S.P.-A.; writing—original draft preparation, C.R. and J.S.P.-A.; writing—review and editing, M.N., A.P., F.G., A.S. and F.Z.; visualization, C.R. and J.S.P.-A.; supervision, M.N. and J.S.P.-A.; project administration, M.N.; funding acquisition, M.N. and J.S.P.-A. All authors have read and agreed to the published version of the manuscript.

**Funding:** C. Ricci was supported by the project “Degrado Urbano” of Fondazione Centro Conservazione e Restauro “La Venaria Reale” (Turin, Italy), funded by the “Compagnia di San Paolo”. J.S. Pozo-Antonio was supported by the Ministry of Economy and Competitiveness, Government of Spain through Grant NO. IJCI-2017-32771.

**Acknowledgments:** This research was performed in the framework of the teaching innovation group *ODS Cities and Citizenship* of University of Vigo (Spain). We also acknowledge A. De Stefanis (Fondazione Centro Conservazione e Restauro “La Venaria Reale”) for her contribution in accomplishing the cleaning tests.

**Conflicts of Interest:** The authors declare no conflict of interest.

## References

1. United Nations. About the Sustainable Development Goals (Agenda 2030). Available online: <https://www.un.org/sustainabledevelopment/sustainable-development-goals/> (accessed on 20 March 2020).
2. ICOMOS. Concept Note for the United Nations Agenda 2030 and the Third United Nations Conference on Housing and Sustainable Urban Development (HABITAT). 2016. Prepared by Hosagrahar, J.; Soule, J.; Fusco Girard, L.; Potts, A.. Available online: <http://www.usicomos.org/wp-content/uploads/2016/05/Final-Concept-Note.pdf> (accessed on 20 March 2020).
3. GRAFFITAGE Project. Development of a New Anti-graffiti System, Based on Traditional Concepts, Preventing Damage of Architectural Heritage Materials. Final Report of the SSP (Policy Oriented Research) of the Sixth European Programme of the European Commission. European Union: Brussels, Belgium, 2008; FP6-2003-SSP 3–513718. Available online: <https://cordis.europa.eu/project/id/513718/reporting> (accessed on 20 March 2020).
4. GRAFFOLUTION Project. Awareness and Prevention Solutions against Graffiti Vandalism in Public Areas and Transport. Final Report of the SSP (Policy Oriented Research) of the Seventh European Programme of the European Commission. European Union: Brussels, Belgium, 2016; FP7-SEC-2013-1. 2016. Available online: <https://cordis.europa.eu/project/id/608152> (accessed on 20 March 2020).
5. Sanmartín, P.; Cappitelli, F.; Mitchell, R. Current methods of graffiti removal: A review. *Constr. Build. Mater.* **2014**, *71*, 363–374. [CrossRef]
6. Pozo-Antonio, J.S.; Rivas, T.; López, A.J.; Fiorucci, M.P.; Ramil, A. Effectiveness of granite cleaning procedures in cultural heritage: A review. *Sci. Total Environ.* **2016**, *571*, 1017–1028. [CrossRef] [PubMed]
7. Gomes, V.; Dionísio, A.; Pozo-Antonio, J.S. Conservation strategies against graffiti vandalism on Cultural Heritage stones: Protective coatings and cleaning methods. *Prog. Org. Coat.* **2017**, *113*, 90–109. [CrossRef]
8. Rivas, T.; Pozo, S.; Fiorucci, M.P.; López, A.J.; Ramil, A. Nd:YVO4 laser removal of graffiti from granite Influence of paint and rock properties on cleaning efficacy. *Appl. Surf. Sci.* **2012**, *263*, 563–572. [CrossRef]
9. Venice Charter for the Conservation and Restoration of Monuments and Sites, ICOMOS. 1964. Available online: <http://www.icomos.org/venicecharter2004/index.html> (accessed on 20 March 2020).
10. Grimmer, A.E. Keeping It Clean: Removing Exterior Dirt, Paint, Stains and Graffiti from Historic Masonry Buildings. In *Library of Congress Cataloging in Publication Data*; Diane Pub Co: Collingdale, PA, USA, 1988. [CrossRef]
11. Historic England. Graffiti on Historic Buildings and Monuments. Methods of Removal and Prevention. 1999, pp. 1–12. Available online: <https://historicengland.org.uk/images-books/publications/graffiti-on-historic-buildings-and-monuments/> (accessed on 20 March 2020).
12. Urquhart, D. The treatment of graffiti on historic surfaces. Advice on graffiti removal procedures, anti-graffiti coatings and alternative strategies. In *Historic Scotland Technical Advice Note*; no.18; TCRE Division/Scottish Conservation Bureau: Edinburgh, Scotland, 1999.
13. Samolik, S.; Walczak, M.; Plotek, M.; Sarzynski, A.; Pluska, I.; Marczak, J. Investigation into the removal of graffiti on mineral supports: Comparison of nano-second Nd:YAG laser cleaning with traditional mechanical and chemical methods. *Stud. Conserv.* **2015**, *60*, 58–64. [CrossRef]
14. Careddu, N.; Akkoyun, O. An investigation on the efficiency of water-jet technology for graffiti cleaning. *J. Cult. Herit.* **2016**, *19*, 426–434. [CrossRef]
15. Gomes, V.; Dionísio, A.; Pozo-Antonio, J.S. The influence of the SO<sub>2</sub> aging on the graffiti cleaning effectiveness with chemical procedures on a granite substrate. *Sci. Total Environ.* **2018**, *625*, 233–245. [CrossRef]
16. Gomes, V.; Dionísio, A.; Pozo-Antonio, J.S.; Rivas, T.; Ramil, A. Mechanical and laser cleaning of spray graffiti paints on a granite subjected to a SO<sub>2</sub>-rich atmosphere. *Constr. Build. Mater.* **2018**, *188*, 621–632. [CrossRef]
17. Pozo-Antonio, J.S.; López, L.; Dionísio, A.; Rivas, T. A Study on the Suitability of Mechanical Soft-Abrasive Blasting Methods to Extract Graffiti Paints on Ornamental Stones. *Coatings* **2018**, *8*, 335. [CrossRef]
18. Fotakis, C.; Anglos, D.; Zafropoulos, V.; Georgiou, S.; Tornari, V. *Lasers in the Preservation of Cultural Heritage: Principles and Applications*; CRC Press, Taylor & Francis Group: Abingdon, Oxfordshire, UK, 2006.
19. Pozo-Antonio, J.S.; Rivas, T.; Fiorucci, M.P.; López, A.J.; Ramil, A. Effectiveness and harmfulness evaluation of graffiti cleaning by mechanical, chemical and laser procedures on granite. *Microchem. J.* **2016**, *125*, 1–9. [CrossRef]



20. Giusti, C.; Colombini, M.P.; Lluveras-Tenorio, A.; La Nasa, J.; Striova, J.; Salvadori, B. Graphic vandalism: Multi-analytical evaluation of laser and chemical methods for the removal of spray paints. *J. Cult. Herit.* **2020**, in press. [CrossRef]
21. Ortiz, P.; Antúnez, V.; Ortiz, R.; Martín, J.M.; Gómez, M.A.; Hortal, A.R.; Martínez-Haya, B. Comparative study of pulsed laser cleaning applied to weathered marble surfaces. *Appl. Surf. Sci.* **2013**, *283*, 193–201. [CrossRef]
22. Costela, A.; García-Moreno, I.; Gómez, C.; Caballero, O.; Sastre, R. Cleaning graffiti on urban buildings by use of second and third harmonic wavelength of a Nd:YAG laser: A comparative study. *Appl. Surf. Sci.* **2003**, *207*, 86–99. [CrossRef]
23. Gómez, C.; Costela, A.; García-Moreno, I.; Sastre, R. Comparative study between IR and UV laser radiation applied to the removal of graffiti on urban buildings. *Appl. Surf. Sci.* **2006**, *252*, 2782–2793. [CrossRef]
24. Pozo-Antonio, J.S.; Papanikolaou, A.; Melessanaki, K.; Rivas, T.; Pouli, P. Laser-Assisted Removal of Graffiti from Granite: Advantages of the Simultaneous Use of Two Wavelengths. *Coatings* **2018**, *8*, 124. [CrossRef]
25. Chapman, S. Laser technology for graffiti removal. *J. Cult. Herit.* **2000**, *1*, 75–78. [CrossRef]
26. Langworth, S.; Anundi, H.; Friis, L.; Johanson, G.; Lind, M.L.; Söderman, E.; Åkesson, B.A. Acute health effects common during graffiti removal. *Int. Arch. Occup. Environ. Health* **2001**, *74*, 213–218. [CrossRef]
27. TriSolv Software, ISCR. Triangolo interattivo dei solventi e delle solubilità®. Available online: <http://icr.beniculturali.it/flash/progetti/TriSolv/TriSolv.html> (accessed on 31 January 2018).
28. Coladonato, M.; Scarpitti, P. Note sul Triangolo interattivo dei solventi e delle solubilità©. 2008. Available online: [http://www.icr.beniculturali.it/flash/progetti/TriSolv/dati/IT/TriSolv\\_IT.pdf](http://www.icr.beniculturali.it/flash/progetti/TriSolv/dati/IT/TriSolv_IT.pdf) (accessed on 31 January 2018).
29. Hansen, C.M. *Hansen Solubility Parameters: A User's Handbook*; CRC Press, Taylor & Francis Group: Abingdon, Oxfordshire, UK, 2007.
30. *Handbook for Critical Cleaning: Cleaning Agents and Systems*; Kanegsberg, B.; Kanegsberg, E. (Eds.) CRC Press, Taylor & Francis Group: Abingdon, Oxfordshire, UK, 2011.
31. Gambino, F.; Borghi, A.; D'Atri, A.; Gallo, L.M.; Ghiraldi, L.; Giardino, M.; Martire, L.; Palomba, M.; Perotti, L. TOURinSTONES: A free mobile application for promoting geological heritage in the city of Turin (NW Italy). *Geoheritage* **2018**, *11*, 3–17. [CrossRef]
32. Sandrone, R.; Colombo, A.; Fiora, A.; Fornaro, L.; Lovera, E.; Tunesi, A.; Cavallo, A. Contemporary natural stones from the Italian western Alps (Piedmont and Aosta Valley Regions). *Per. Mineral.* **2004**, *73*, 211–226.
33. ASTM-D4404-10. *Standard Test Method for Determination of Pore Volume and Pore Volume Distribution of Soil and Rock by Mercury Intrusion Porosimetry*; ASTM International: West Conshohocken, PA, USA, 2010.
34. Montana Colors. Available online: [www.montanacolors.com](http://www.montanacolors.com) (accessed on 31 January 2017).
35. U.S. National Library of Medicine. National Center for Biotechnology Information. Available online: <https://pubchem.ncbi.nlm.nih.gov/> (accessed on 31 January 2018).
36. CIE0144 S–S/E:2007 *Colorimetry Part 4: CIE 1976 L\*a\*b\* Color Space*; CIE Central Bureau: Vienna, Austria, 2007.
37. Prieto, B.; Sanmartín, P.; Silva, B.; Martínez-Verdú, F. Measuring the color of granite rocks. A proposed procedure. *Color Res. Appl.* **2010**, *35*, 368–375. [CrossRef]
38. UNI-EN ISO 4288:1996 *Geometrical Product Specifications (GPS)—Surface Texture: Profile Method—Rules and Procedures for the Assessment of Surface Texture*; International Organization for Standardization: Geneva, Switzerland, 1996.
39. Cremonesi, P. *L'uso dei Solventi Organici nella Pulitura di Opere Policrome*; IL PRATO PUBLISHING HOUSE SRL: Saonara, Italy, 2004.
40. Mokrzycki, W.S.; Tatol, M. Color difference DE—A survey. *Mach. Graph. Vis.* **2011**, *20*, 383–411.
41. Rodrigues, J.D.; Grossi, A. Indicators and ratings for the compatibility assessment of conservation actions. *J. Cult. Herit.* **2007**, *8*, 32–43. [CrossRef]
42. Hanaor, D.A.H.; Sorrell, C.C. Review of the anatase to rutile phase transformation. *J. Mater. Sci.* **2011**, *46*, 855–874. [CrossRef]
43. Abel, A. Pigments for paints. In *Paints in Surface Coatings: Theory and Practice*; Lambourne, R., Strivens, T.A., Eds.; Woodhead Publishing: Cambridge, UK, 1999.
44. Diebold, M.P. Optimizing the benefits of TiO<sub>2</sub> in paints. *J. Coat. Technol. Res.* **2020**, *17*, 1–17. [CrossRef]
45. Zhou, D.; Ji, Z.; Jiang, X.; Dunphy, D.R.; Brinker, J.; Keller, A.A. Influence of material properties on TiO<sub>2</sub> nanoparticle agglomeration. *PLoS ONE* **2013**, *8*, 1–7. [CrossRef]

46. Rodrigues, J.D.; Costa, D.; Mascalchi, M.; Osticioli, I.; Siano, S. Laser ablation of iron-rich black films from exposed granite surfaces. *Appl. Phys. A* **2014**, *117*, 365–370. [[CrossRef](#)]
47. Ramil, A.; Pozo-Antonio, J.S.; Fiorucci, M.P.; López, A.J.; Rivas, T. Detection of the optimal laser fluence ranges to clean graffiti on silicates. *Constr. Build. Mater.* **2017**, *148*, 122–130. [[CrossRef](#)]
48. Kliem, W.; Lehmann, G. A reassignment of the optical absorption bands in biotites. *Phys. Chem. Miner.* **1979**, *4*, 65–75. [[CrossRef](#)]



© 2020 by the authors. Licensee MDPI, Basel, Switzerland. This article is an open access article distributed under the terms and conditions of the Creative Commons Attribution (CC BY) license (<http://creativecommons.org/licenses/by/4.0/>).